HHS Public Access

Author manuscript

AJNR Am J Neuroradiol. Author manuscript; available in PMC 2017 June 01.

Published in final edited form as:

AJNR Am J Neuroradiol. 2016 December ; 37(12): 2273–2279. doi:10.3174/ajnr.A4886.

Metabolic Abnormalities in the Hippocampus of Patients with Schizophrenia: A 3D Multivoxel MR Spectroscopic Imaging Study at 3 T

Emma J. Meyer, MD[1], **Ivan I. Kirov, PhD**[1], **Assaf Tal, PhD**[2], **Matthew S. Davitz, BS**[1], **James Babb, PhD**[1], **Mariana Lazar, PhD**[1], **Dolores Malaspina, MD**[3], and **Oded Gonen, PhD**[1]

[1]Center for Advanced Imaging Innovation and Research (CAI[2]R), Bernard and Irene Schwartz Center for Biomedical Imaging, Department of Radiology, NYU School of Medicine, New York, 10016 USA

[2]Department of Chemical Physics, The Weizmann Institute of Science, Rehovot 7610001, Israel

[3]Institute for Social and Psychiatric Initiatives (InSPIRES), Department of Psychiatry, New York, NY, 10016 USA

Abstract

BACKGROUND AND PURPOSE—Schizophrenia is well known to be associated with hippocampal structural abnormalities. We used ^{1}H-MRS imaging to test the hypothesis that these abnormalities are accompanied by NAA deficits, reflecting neuronal dysfunction, in patients compared with healthy controls.

MATERIALS AND METHODS—Nineteen patients with schizophrenia (11 male, 40.6±10.1 years old, 19.5±10.5 years disease duration) and 11 matched healthy controls (5 male, 33.7±10.1 years old) underwent MRI and multi-voxel point resolved spectroscopy (TE/TR=35/1400 ms) ^{1}H-MRS imaging at 3 T to obtain their hippocampal GM absolute NAA, Cr, Cho and mIns concentrations. Unequal variance *t*-tests and ANCOVA were used to compare patients with controls. Bilateral volumes from manually outlined hippocampal masks were compared using unequal variance *t*-test.

RESULTS—Patients' average hippocampal GM Cr concentration was 19% higher than controls', 8.7±2.2 versus 7.4±1.2 mM (p<0.05); with no differences in NAA: 8.8±1.6 *vs.* 8.7±1.2 mM, Cho: 2.3±0.7 *vs.* 2.1±0.3 mM, or mIns: 6.1±1.5 *vs.* 5.2±0.9 (all p>0.1). There was a positive correlation between mIns and Cr in patients (r=0.57, p=0.05) but not controls. Bilateral hippocampal volume was ~10% lower in patients: 7.5±0.9 *vs.* 8.4±0.7 cm^3 (p<0.05).

Corresponding Author/Reprints requests: Oded Gonen, PhD, Department of Radiology, New York University School of Medicine, 660 First Avenue, 4-th Floor, New York, NY 10016, Telephone: (212) 263-3532, FAX: (212) 263-7541, oded.gonen@med.nyu.edu.

DISCLOSURES: Emma Meyer—*RELATED:* NIH.* **Ivan Kirov**—*UNRELATED: Travel/Accommodations/Meeting Expenses Unrelated to Activities Listed:* North American Brain Injury Society, Comments: For travel to their annual meeting with the purpose of giving a lecture on proton MR spectroscopy in traumatic brain injury. **Mariana Lazar**—*RELATED: Grant:* National Institute of Mental Health,* Comments: This work was funded in part by a grant from National Institute of Mental Health. **Dolores Malaspina**—*RELATED: Grant:* NIMH*; *UNRELATED: Expert Testimony:* Total in career of 10,000, Comments: As a psychiatrist, I consult on issues such as psychiatric diagnoses by mass shooters, possible mental illness in transportation agents; *Grants/Grants Pending:* NIMH.*

*money paid to institution

CONCLUSION—These findings suggest that the hippocampal volume deficit in schizophrenia is not due to net loss of neurons, in agreement with histopathology studies but not with prior ^{1}H-MRS reports. Elevated Cr is consistent with hippocampal hypermetabolism and its correlation with mIns may also suggest an inflammatory process affecting some cases; this may suggest treatment targets and markers to monitor them.

INTRODUCTION

Schizophrenia (SZ) is a chronic psychiatric disorder that profoundly alters a person's perception, cognition, and behavior. Due to its high prevalence, ~1%, early onset and the limited efficacy of existing treatments, SZ exacts enormous personal and economic toll (1). The characteristic “positive” symptoms of SZ psychosis (delusions, hallucinations, disorganized speech and behavior) are accompanied by cognitive decline and “negative” symptoms including diminished emotional expression and avolition (2). Despite recognition as fundamental to the disorder as early as 1919, cognitive and negative symptoms were largely ignored once relatively effective pharmacological treatments for the positive symptoms emerged in the 1950s (3). In recent years, development of sophisticated investigative techniques has rekindled interest in the neurobiological substrate underlying SZ such that therapy may be developed to target the full range of symptoms and alter the clinical course.

This surge of effort has resulted in the development of a plurality of sometimes competing, sometimes overlapping theories of SZ pathophysiology, from the classic neurotransmitter-based theories to genetic, immune, synapse, and network-based theories. The hippocampus is implicated in many of these. SZ is known to be associated with reduced hippocampal volume, increased basal perfusion, decreased activation during certain memory tasks, decreased neurogenesis in its dentate gyrus and reduced connectivity with cortical and subcortical regions (4–9). Recent findings show that conversion to psychosis in high-risk subjects is predicted by hypermetabolism in the hippocampal CA1 subregion (4). Psychosis may be conceptualized as a disruption in learning and memory involving impaired habituation and “runaway” pattern completion due to hippocampal hyperactivity (4, 10, 11). The mechanism underlying these hippocampal abnormalities remain unclear. The absence of gliosis on post-mortem histopathology and reduced volume in prodromal and first-episode cases has fomented a shift from neuro-degenerative to neuro-developmental hypotheses (12). Lack of classic neurodegeneration with gliosis, however, does not imply absence of subtler progressive damage and inflammation. Mounting genetic and epidemiological data suggests a role for aberrant immune function and inflammation in SZ (13).

^{1}H-MRS measures metabolites used as markers for underlying physiologic processes. Most prominently: NAA (NAA and *N*-acetylaspartylglutamate) for neuronal integrity, Cr (creatine and phosphocreatine) for energy metabolism, Cho (phosphocholine, choline and glycerophosphocholine) for membrane turnover and mIns (myo-inositol) for astroglial proliferation. (14). Most previous hippocampal ^{1}H-MRS studies in SZ report lower NAA (15); one found increased Cr and Cho (15). None of ten others that measured Cho, seven Cr, or eight mIns, found changes (16). Difficulty interpreting results may stem from diagnostic

heterogeneity within and between studies, insufficiently powered samples and methodological variation (16).

This study compares absolute hippocampal GM NAA, Cr, Cho and mIns levels, obtained with three-dimensional (3D) multivoxel ^{1}H-MRS (^{1}H-MRSI) at 3 T, between SZ patients and controls in order to test the hypothesis that the former have decreased hippocampal GM NAA reflecting neuronal damage. Higher field strength and ^{1}H-MRSI (compared with single-voxel) yield better coverage of the hippocampus's irregular shape, better SNR and spatial resolution.

MATERIALS AND METHODS

I. Human Subjects

The SZ or schizoaffective disorder cases were recruited from the outpatient clinics of NYU Langone Medical Center and Bellevue Hospital, diagnosed based on the Diagnostic Interview for Genetic Studies conducted by clinicians trained to reliability, and had ongoing assessments (17). All were taking stable doses of medications and had no other psychiatric or neurological disorders. Age-matched controls recruited from hospital postings met the criteria of no personal or family history of psychosis, no Axis I disorder in the last two years, and no known neurological disorder. Exclusion criteria for both cases and controls included uncontrolled medical illness, MRI contraindication or inability to tolerate MR exam and substance (except tobacco) use in the past six months. Substance use history of the cases, is: 6/19 reported current or past tobacco use, 6/19 past cannabis, 9/19 past cocaine, and 7/19 reported past alcohol use. All participants demographics are compiled in Table 1 and all gave Institutional Review Board approved written consent.

II. MR Data Acquisition

All experiments were done at 3 T in a whole body MRI scanner (Trio, Siemens AG, Erlangen Germany) using a transmit-receive head-coil (TEM3000, MR Instruments, Minneapolis, MN). For anatomic reference, tissue segmentation and ^{1}H-MRSI VOI guidance, T1-weighted, 3D MPRAGE images were obtained from each subject: TE/TI/TR=2.6/800/1360 ms, 256×256 matrix, 256×256 mm^{2} field-of-view (FOV), 160 slices, 1 mm thick each. These were reformatted into 192 axial, sagittal and coronal slices at 1 mm^{3} isotropic resolution.

Our non-iterative, $\mathbf{B_0}$ map based, Bolero (B0 loop encoded readout) software adjusted the scanner's 1st and 2nd order shims to optimize the magnetic field homogeneity over the hippocampi in 3–5 minutes (18). A 6 cm anterior-posterior (AP) ×9 cm left-right (LR) ×2 cm inferior-superior (IS)=108 cm^{3} parallelepiped ^{1}H-MRSI VOI was then image guided over the bilateral hippocampus, as shown in Fig. 1. This VOI was excited using point resolved spectroscopy (*TE/TR*= 35/1400 ms) with two 2nd-order Hadamard encoded slabs (4 slices) interleaved along the IS direction every *TR*, as shown in Fig. 1**b**, for optimal SNR and spatial coverage (19). Interleaving also enabled strong, 9 mT/m, Hadamard slice-selection gradients reducing the NAA → mIns chemical shift displacement to ~0.13 mm, ~3% of the slice thickness (20). Thin slices were also chosen to reduce broadening from

susceptibility gradients in the IS direction from the air-tissue interface with the maxillary sinuses just below, as seen in Fig. 1**a**.

The four Hadamard slices' planes were encoded with 16×16 2D-CSI over a 16×16 cm^2 (LR×AP) FOV to form 1.0×1.0×0.5 cm^3 voxels. [Note that the actual voxel size (=full width at half maximum of the point spread function) for such uniform 2D phase encoding is 1.12×1.12×0.5=0.63 cm^3 (21, 22), since in the Hadamard direction the nominal equals the actual voxel size (23)]. The VOI was defined in their planes by two 11.2 ms numerically optimized 180° RF pulses (4.8 kHz bandwidth) under 1.8 and 1.2 mT/m in the AP and LR directions, to yield 9×6×4=216 voxels (see Fig. 1**c**). Such gradients lead the NAA VOI to experience a relative slice in-plane chemical shift displacement of 2.3 mm in the AP and 3.5 mm in the LR directions (24), *i.e.,* of the 6×9×2 cm^3 AP×LR×IS nominal VOI, at least 5.7×8.6×2 cm^2 (93.4%) is common for all metabolites (25). Note *(i)* the Cho and Cr suffer even smaller relative displacements; *(ii)* the CSI localization grid does not experience this displacement (26); *(iii)* because it is a relative shift, this error is encountered *only* at the VOI edges (25).; and *(iv)* it is smaller than the 1×1 cm^2 in-plane CSI resolution. Therefore, to avert it for all metabolites, we chose the in-plane VOI size large enough, 9×6 cm^2, to have these displacement-error prone voxels at the VOI-edges completely outside the hippocampus, as shown in Fig. 1**a** and 2**a**. The MRS signals were acquired for 256 ms at ±1 kHz bandwidth. At two averages the ^{1}H-MRS was ~25 minutes and the exam took under an hour.

III. MRS Post Processing

The MRS data were processed offline using in-house software. Residual water was removed from the MR signals in the time domain (27), the data static-field drift corrected (28), voxel-shifted to align the CSI grid with the NAA VOI, Fourier transformed in the temporal, AP and LR direction and Hadamard reconstructed along the IS. Spectra were automatically corrected for frequency and zero-order phase shifts in reference to the NAA peak in each voxel.

Relative levels of the i^{th} (i=NAA, Cr, Cho, mIns) metabolite in the j^{th} (j=1..216) voxel of the k^{th} (k=1..30) subject were estimated from their peak area, S_{ijk}, using parametric spectral modeling (29), with Glx, Cho, Cr, *m*I, NAA and taurine model functions, as shown in Fig. 1**d**. The S_{ijk} were scaled into absolute concentration, C_{ijk}, relative to a 2 L reference sphere of C_i^{vitro}=12.5, 10.0, 3.0 and 7.5 mM NAA, Cr, Cho and mIns in water at physiological ionic strength:

$$C_{ijk}=C_i^{\text{vitro}}\cdot\frac{S_{ijk}}{S_{ijR}}\cdot\frac{V_k^{180^\circ}}{V_R^{180^\circ}}\cdot\frac{1}{F_{jk}}\cdot f_i, \quad [1]$$

where S_{ikR} is the phantom's metabolites' signals; and $V_j^{180^\circ}, V_R^{180^\circ}$ subject and reference RF voltages for non-selective 1 ms 180° pulses and F_{jk} is that voxels tissue fraction, estimated from the WM, GM and CSF segmented MP-RAGE images, as described below. The f_i

corrects C_{ijk} for *in vivo* ($T_1^{\text{vivo}}, T_2^{\text{vivo}}$ assuming small patients-controls differences) and *in vitro* ($T_1^{\text{vitro}}, T_2^{\text{vitro}}$) relaxation times differences (30):

$$f_i = \frac{\exp\ (-TE/T_2^{\text{vitro}})}{\exp\ (-TE/T_2^{\text{vivo}})} \cdot \frac{1-\exp\ (-TR/T_1^{\text{vitro}})}{1-\exp\ (-TR/T_1^{\text{vivo}})}. \quad [2]$$

using the T_1^{vivo}=1.4, 1.3, 1.1 and 1.2 s, T_2^{vivo}=343, 172, 248 and 200 ms reported for NAA, Cr, Cho and mIns at 3 T (31–33); and T_1^{vitro}=605, 336, 235 and 319 ms, T_2^{vitro}=483, 288, 200 and 233 ms in the reference phantom.

Bilateral hippocampi masks were manually traced on the axial MP-RAGE images based on an MRI atlas (34), as shown in Fig. 1**a**, and visually verified on sagittal and coronal planes. The axial MRI were segmented into CSF, gray and white matter (GM, WM) masks using SPM12 [University College London, UK (35)], as shown in Fig. 2**b**–**d**. An in-house program (MATLAB 14, Mathworks, Framingham, MA) calculated the fraction of each tissue mask inside each voxel (36), from which F_{jk} = (GM volume+ WM volume)/ (voxel volume) for Eq. [1] was obtained. We retained only voxels with at least 30% their volume within the hippocampus mask. To minimize inclusion of degraded signals, only voxels that also had: *(i)* F_{jk} >70%, *i.e.,* contained <30% CSF, *(ii)* Cramer-Rao lower bounds <20% for a given metabolite; and *(iii)* 4 Hz< linewidths <13 Hz, were retained, as shown in Fig. 2. The software then estimated the global GM and WM concentrations of each metabolite in the retained $N \geq 2$ hippocampus voxels using linear regression, as described previously (36). This approach overcomes the GM/WM partial volume issue encountered by single-voxel MRS. Note that although metabolic gradients are reported along the long axis of the hippocampus (37, 38), since the entire structure is taken here as a whole; and these metabolites' *intra*-subject gradients are reported to be quite similar, our *average* concentration reported here is nevertheless a useful *inter*-subject comparison metric.

IV. Statistical Analyses

Exact Mann-Whitney and unequal variance *t*-tests were used to compare the groups in terms of age and in terms of the volume measure and each metabolite concentration without adjustment for age and gender. ANOVA was used to compare the groups in terms of the volume and each metabolite concentration adjusted for age and gender. ANOVA for each measure allowed the error variance to differ across subject groups to avoid an assumption of variance equality. F and Levene tests were used to compare the groups in terms of the variance of the volume measure and each metabolite concentration. All tests were conducted at the 5% significance level.

RESULTS

A total of 19 cases and 11 controls were included in the analyses, as shown in Table 1. The groups were not different with respect to age (p=0.119). The Bolero shim procedure yielded metabolites linewidths of 8.1±3.0 Hz across all 216 VOI voxels for patients and controls, as shown in Fig. 1. The number of voxels that passed the selection criteria described above and

were used to estimate metabolites' concentrations were 10.5±3.4 in patients and 14.5±5.4 in controls for NAA; 8.3±3.4 and 11.3±4.9 for Cho; 8.0±3.5 and 12.8±4.4 for Cr; 4.8±1.7 and 7.0±3.8 for mIns. Average hippocampal GM metabolite concentrations and the bilateral volumes, as shown in Fig. 1**a**, are given in Table 2. Note that since the analysis was done independently for each metabolite, different numbers of subjects are included for each, based on how many had at least two voxels that passed the exclusion criteria.

Patients had 19% ($p<0.05$) higher hippocampal GM Cr level than controls, even after adjusting for age and gender, as shown in Table 2 and Fig. 3. NAA, Cho and mIns were not significantly different. The variance of the Cho levels was larger in patients than in controls ($p=0.05$); and trended that way in Cr ($p=0.06$). There was a positive correlation between mIns and Cr levels in patients (r=0.57, $p=0.05$) but not in controls (r=0.42, $p=0.26$). Other metabolites were not significantly correlated. Bilateral hippocampal volume was ~10% ($p<0.05$) lower in patients.

DISCUSSION

Surprisingly, our findings do *not* support the hypothesis that patients with SZ exhibit decreased hippocampal GM NAA (due to neuronal dysfunction) compared with healthy controls, as generally reported (16). They are, however, concordant with neuropathology studies that consistently find reduced hippocampal volume without net loss of neurons, but with neuronal architectural disarray and molecular alterations, *e.g.,* changes in receptor density and deficits in the inhibitory interneurons that comprise 10% of hippocampal neurons (12).

Our finding of elevated hippocampal GM Cr in SZ may suggest either altered hippocampal energy metabolism or increased proportion of glial cells. The is because the Cr ^{1}H-MRS peak is a composite of free creatine and phosphocreatine that interconvert to regenerate ATP, thus acting as a short-term energy “buffer” for the cell. Cr elevation may, therefore, reflect altered energy metabolism, likely *hyper*-metabolism as a more metabolically active cell reasonably requires greater capacity to regenerate ATP (decreased Cr has similarly been interpreted as *hypo*-metabolism) (10, 39). Indeed, increase in energy metabolism is consistent with the hippocampal hyperactivity model of SZ, supported by evidence from animal model, neuroimaging and histopathology studies (40). Nuclear imaging studies show increased basal perfusion (41) that correlates with psychotic symptoms and is normalized by D2 antagonists (42), while resting state fMRI shows hyperactivity correlated with cognitive deficits and negative symptoms (43). Hippocampal hyperactivity may be mediated by increased glutamatergic activity, which has been found in the hippocampus of unmedicated SZ patients and associated with reduced hippocampal volume and worse executive functioning and global clinical state (44). Furthermore, a reciprocal pathway between the hippocampus and dopaminergic neurons in the midbrain supports a link to the dopamine hypothesis of SZ (40).

Cho and mIns are elevated alongside Cr in astrogliosis, reflecting their higher levels in glial cells than neurons (14). Although we did not find significant elevations in hippocampal GM Cho or mIns, the correlation between Cr and mIns in cases (but not controls) suggests that in

at least some cases elevation in Cr may reflect astrogliosis - a response to inflammation. Evidence supporting an immune or inflammatory component in SZ continues to accumulate. This includes the increased risk of SZ after exposure to certain maternal viruses *in utero*, the increased expression in the hippocampus of genes related to the immune response identified by mRNA sequencing, the significant associations with inflammatory-related genes identified in GWAS meta-analyses (including in the HLA complex, where a recent study suggests increased expression of a complement component gene may mediate excessive synaptic pruning), and the increase in proinflammatory cytokines including IL-6 and TNF-α in patients with psychosis (45, 46).

That histopathology studies do not show glial cell proliferation in SZ does not rule out the possibility that a subset of patients undergo astrogliosis (12). This notion is consistent with the emerging concept of the clinical syndrome of SZ as composed of a group of separate conditions differing in relevant pathophysiologies, termed “SZ and related psychoses”. Consistent with the idea of etiological heterogeneity, cases exhibited greater coefficients of variation than controls for both Cho (28% *vs.* 16%, p=0.05) and Cr (25% *vs.* 16%, p=0.06). A subset of cases may undergo an inflammatory process, causing elevated Cho, Cr, and mIns through astrogliosis or subtler inflammation that damages glial cells and/or myelin.

The reduced hippocampal volume seen in patients is consistent with prior reports. Along with the prefrontal cortex, the hippocampus is consistently observed to undergo volume loss in SZ (4). A recent collaborative analysis of brain volumes using imaging data from 2028 individuals with SZ and 2540 healthy controls found the largest patient control effect size for the hippocampus of any subcortical area, with a mean 4.10% volume decrease compared with controls (47). The lack of correlation between hippocampal volume and NAA level in our study suggests that the lower volume in patients is not due to neuronal loss from progression of a pathogenic process and may, therefore, be suggestive of a developmental trait.

There may be several reasons for the discordance between our findings and most previous studies. First, clinical heterogeneity (disease duration, symptomatology, medications) both between and within studied populations is known to affect ^{1}H-MRS results (16). Second, methodology differences are well-known to affect results. Our 3D technique yields better spatial resolution (0.5 cm^3 versus 3.5 cm^3 or larger) and delineation of the irregular shape, with less inclusion of neighboring WM than single-voxels, even accounting for partial WM and CSF volume. Third, studies that found lower NAA in patients had on average longer TEs, making them more sensitive to quantification errors due to T_2-weighting variations, than our short, TE=35 ms acquisition (48). Fourth, some studies use Cr as an “internal reference” and report its ratios with other metabolites. This approach magnifies errors and is further complicated by findings that Cr is altered in several brain regions in SZ (16). Finally, as others point out, there is a publication bias in favor of NAA deficit reports as opposed to a finding of “no change” (16).

Admittedly, our study also has several limitations. First, our sample comprised patients with varying disease durations, medication regimens, and history of substance use at insufficient numbers to distinguish the effect of these variables. Second, a relatively small sample size

may have limited the power to detect small differences, *e.g.,* Cho or mIns elevations in the patients. Third, even our improved spatial resolution is insufficient to resolve hippocampal subfields that may be differentially affected in SZ (4). Third, the regressions used to obtain metabolites' concentrations relied on relatively few, 8 – 14 voxels per individual, as a balance was struck between the 3D ^{1}H-MRSI spatial resolution, measurement time and hippocampus volume. While this may be improved at higher fields, at 3 T, this is likely nearly as good as can be achieved. Fourth, because of the anatomical milieu (deep in the brain, irregularly shaped, near air filled sinuses), it is difficult to obtain adequate SNR to quantify hippocampal glutamate and glutamine levels. Finally, our interpretation of elevated Cr is limited by the inability of 3 T ^{1}H-MRS to distinguish the Cr from phosphocreatine resonances, and our proposals of altered energy metabolism and astrogliosis are here supported by inference and existing literature rather than direct measurement.

CONCLUSIONS

Decreased volume without GM NAA decline in the hippocampus of patients with SZ suggests a process that preserves neuronal integrity and could represent a developmental rather than pathological disruption. Increased hippocampal GM Cr suggests hypermetabolism and/or possibly astrogliosis in a subset of patients. These findings may have implications for both the pathogenesis and treatment of SZ by supporting the hippocampal hyperactivity model. In some patients an inflammatory process (possibly involving astrogliosis) may be a treatment target in addition to the anti-dopaminergic treatments. Indeed, there is growing recognition that the efficacy of antipsychotics may be mediated in part through anti-inflammatory action and there are ongoing efforts with promising results using anti-inflammatory agents including aspirin, COX-2 inhibitors and *N*-acetylcysteine as adjuvant therapies (49). Therefore, we propose ^{1}H-MRSI both as a probe to identify patient subgroups and as a method to monitor therapies.

Acknowledgments

Funding

This work was supported by NIH grants: RC1MH088843, 2K24MH00169, MH108962, EB011639, EB01015, NS081772, NS090417, NS097494; and the Center for Advanced Imaging Innovation and Research (CAI^{2}R, www.cai2r.net), a NIBIB Biomedical Technology Resource Center (NIH P41 EB017183) and CTSI UL1TR000038 (NYU). Assaf Tal acknowledges the support of the Monroy-Marks Career Development Fund, the Carolito Stiftung Fund, the Leona M. and Harry B. Helmsley Charitable Trust and the historic generosity of the Harold Perlman Family. This research was supported by a research grant from the Sylvia Schaefer Alzheimer's Research Fund.

Abbreviation Key

SZ	schizophrenia
^{1}H-MRSI	three dimensional multivoxel ^{1}H-MRS

REFERENCES

1. Wu EQ, Birnbaum HG, Shi L, et al. The economic burden of schizophrenia in the United States in 2002. J Clin Psychiatry. 2005; 66:1122–1129. [PubMed: 16187769]

2. American Psychiatric Association. Diagnostic and statistical manual of mental disorders : DSM-5. Washington, D.C.: American Psychiatric Association; 2013. American Psychiatric Association. DSM-5 Task Force.

3. Malaspina D, Walsh-Messinger J, Gaebel W, et al. Negative symptoms, past and present: a historical perspective and moving to DSM-5. Eur Neuropsychopharmacol. 2014; 24:710–724. [PubMed: 24314851]

4. Tamminga CA, Stan AD, Wagner AD. The hippocampal formation in schizophrenia. Am J Psychiatry. 2010; 167:1178–1193. [PubMed: 20810471]

5. Adriano F, Caltagirone C, Spalletta G. Hippocampal volume reduction in first-episode and chronic schizophrenia: a review and meta-analysis. Neuroscientist. 2012; 18:180–200. [PubMed: 21531988]

6. Steen RG, Mull C, McClure R, Hamer RM, Lieberman JA. Brain volume in first-episode schizophrenia: systematic review and meta-analysis of magnetic resonance imaging studies. Br J Psychiatry. 2006; 188:510–518. [PubMed: 16738340]

7. Iritani S. Neuropathology of schizophrenia: a mini review. Neuropathology. 2007; 27:604–608. [PubMed: 18021384]

8. Samudra N, Ivleva EI, Hubbard NA, et al. Alterations in hippocampal connectivity across the psychosis dimension. Psychiatry Res. 2015

9. Kirov II, Hardy CJ, Matsuda K, et al. In vivo 7 Tesla imaging of the dentate granule cell layer in schizophrenia. Schizophr Res. 2013; 147:362–367. [PubMed: 23664589]

10. Wood SJ, Berger G, Velakoulis D, et al. Proton magnetic resonance spectroscopy in first episode psychosis and ultra high-risk individuals. Schizophr Bull. 2003; 29:831–843. [PubMed: 14989417]

11. Schobel SA, Lewandowski NM, Corcoran C, et al. The CA1 subfield is a primary site of hippocampal dysfunction associated with Schizophrenia. Archives of General Psychiatry. 2009 In Press.

12. Harrison PJ. The hippocampus in schizophrenia: a review of the neuropathological evidence and its pathophysiological implications. Psychopharmacology (Berl). 2004; 174:151–162. [PubMed: 15205886]

13. Najjar S, Pearlman DM, Alper K, Najjar A, Devinsky O. Neuroinflammation and psychiatric illness. J Neuroinflammation. 2013; 10:43. [PubMed: 23547920]

14. Zhu H, Barker PB. MR spectroscopy and spectroscopic imaging of the brain. Methods Mol Biol. 2011; 711:203–226. [PubMed: 21279603]

15. Lutkenhoff ES, van Erp TG, Thomas MA, et al. Proton MRS in twin pairs discordant for schizophrenia. Mol Psychiatry. 2010; 15:308–318. [PubMed: 18645571]

16. Schwerk A, Alves FD, Pouwels PJ, van Amelsvoort T. Metabolic alterations associated with schizophrenia: a critical evaluation of proton magnetic resonance spectroscopy studies. J Neurochem. 2014; 128:1–87. [PubMed: 23937509]

17. Nurnberger JI Jr, Blehar MC, Kaufmann CA, et al. Diagnostic interview for genetic studies. Rationale, unique features, and training. NIMH Genetics Initiative. Arch Gen Psychiatry. 1994; 51:849–859. discussion 863-844. [PubMed: 7944874]

18. Hetherington HP, Chu WJ, Gonen O, Pan JW. Robust fully automated shimming of the human brain for high-field (1)H spectroscopic imaging. Magn Reson Med. 2006; 56:26–33. [PubMed: 16767750]

19. Goelman G, Liu S, Hess D, Gonen O. Optimizing the efficiency of high-field multivoxel spectroscopic imaging by multiplexing in space and time. Magn Reson Med. 2006; 56:34–40. [PubMed: 16767711]

20. Goelman G, Liu S, Fleysher R, Fleysher L, Grossman RI, Gonen O. Chemical-shift artifact reduction in Hadamard-encoded MR spectroscopic imaging at high (3T and 7T) magnetic fields. Magn Reson Med. 2007; 58:167–173. [PubMed: 17659608]

21. Mareci T, Brooker H. Essential considerations for spectral localization using indirect gradient encoding of spatial information. J Magn Reson. 1991; 92:229–246.

22. Brooker HR, Mareci TH, Mao JT. Selective Fourier transform localization. Magn Reson Med. 1987; 5:417–433. [PubMed: 3431402]

23. Goelman G, Liu S, Gonen O. Reducing voxel bleed in Hadamard-encoded MRI and MRS. Magn Reson Med. 2006; 55:1460–1465. [PubMed: 16685718]

24. de Graaf, RA. in vivo NMR Spectroscopy. Chichester, England: John Weily & Sons; 2007.
25. Barker, PB.; Bizzi, A.; Stefano, ND.; Gullapalli, RP.; Lin, DDM. Clinical MR Spectroscopy Techniques and Applications. Cambridge, New York: Cambridge University Press; 2010. Spectral Analysis Methods, Quantitation and Common Artifacts; p. 34-50.
26. Brown TR, Kincaid BM, Ugurbil K. NMR chemical shift imaging in three dimensions. Proc Natl Acad Sci U S A. 1982; 79:3523–3526. [PubMed: 6954498]
27. Marion D, Ikura M, Bax A. Improved solvent suppression in one- and two-dimensional NMR spectra by convolution of time domain data. J Magn Reson. 1989; 84:425–430.
28. Tal A, Gonen O. Localization errors in MR spectroscopic imaging due to the drift of the main magnetic field and their correction. Magn Reson Med. 2013; 70:895–904. [PubMed: 23165750]
29. Soher BJ, Young K, Govindaraju V, Maudsley AA. Automated spectral analysis III: application to in vivo proton MR spectroscopy and spectroscopic imaging. Magn Reson Med. 1998; 40:822–831. [PubMed: 9840826]
30. Kirov I, George IC, Jayawickrama N, Babb JS, Perry NN, Gonen O. Longitudinal inter- and intra-individual human brain metabolic quantification over 3 years with proton MR spectroscopy at 3 T. Mag Reson Med. 2012; 67:27–33.
31. Traber F, Block W, Lamerichs R, Gieseke J, Schild HH. 1H metabolite relaxation times at 3.0 tesla: Measurements of T1 and T2 values in normal brain and determination of regional differences in transverse relaxation. J Magn Reson Imaging. 2004; 19:537–545. [PubMed: 15112302]
32. Kirov I, Fleysher L, Fleysher R, Patil V, Liu S, Gonen O. Age dependence of regional proton metabolites T2 relaxation times in the human brain at 3 T. Magn Reson Med. 2008; 60:790–795. [PubMed: 18816831]
33. Posse S, Otazo R, Caprihan A, et al. Proton echo-planar spectroscopic imaging of J-coupled resonances in human brain at 3 and 4 Tesla. Mag Reson Med. 2007; 58:236–244.
34. Oishi, K. MRI atlas of human white matter. Amsterdam: Elsevier/Academic Press; 2011.
35. Ashburner J, Friston KJ. Unified segmentation. Neuroimage. 2005; 26:839–851. [PubMed: 15955494]
36. Tal A, Kirov I, Grossman RI, Gonen O. The role of gray and white matter segmentation in quantitative proton MR spectroscopic imaging. NMR Biomed. 2012; 25:1392–1400. [PubMed: 22714729]
37. King KG, Glodzik L, Liu S, Babb JS, de Leon MJ, Gonen O. Anteroposterior hippocampal metabolic heterogeneity: three-dimensional multivoxel proton 1H MR spectroscopic imaging--initial findings. Radiology. 2008; 249:242–250. [PubMed: 18695208]
38. Vermathen P, Laxer KD, Matson GB, Weiner MW. Hippocampal structures: anteroposterior N-acetylaspartate differences in patients with epilepsy and control subjects as shown with proton MR spectroscopic imaging. Radiology. 2000; 214:403–410. [PubMed: 10671587]
39. Mazgaj R, Tal A, Goetz R, et al. Hypo-metabolism of the rostral anterior cingulate cortex associated with working memory impairment in 18 cases of schizophrenia. Brain Imaging Behav. 2015
40. Heckers S, Konradi C. GABAergic mechanisms of hippocampal hyperactivity in schizophrenia. Schizophr Res. 2015; 167:4–11. [PubMed: 25449711]
41. Malaspina D, Storer S, Furman V, et al. SPECT study of visual fixation in schizophrenia and comparison subjects. Biol Psychiatry. 1999; 46:89–93. [PubMed: 10394477]
42. Lahti AC, Holcomb HH, Weiler MA, Medoff DR, Tamminga CA. Functional effects of antipsychotic drugs: comparing clozapine with haloperidol. Biol Psychiatry. 2003; 53:601–608. [PubMed: 12679238]
43. Tregellas JR, Smucny J, Harris JG, et al. Intrinsic hippocampal activity as a biomarker for cognition and symptoms in schizophrenia. Am J Psychiatry. 2014; 171:549–556. [PubMed: 24435071]
44. Poels EM, Kegeles LS, Kantrowitz JT, et al. Glutamatergic abnormalities in schizophrenia: a review of proton MRS findings. Schizophr Res. 2014; 152:325–332. [PubMed: 24418122]
45. Sekar A, Bialas AR, de Rivera H, et al. Schizophrenia risk from complex variation of complement component 4. Nature. 2016; 530:177–183. [PubMed: 26814963]

46. Hwang Y, Kim J, Shin JY, et al. Gene expression profiling by mRNA sequencing reveals increased expression of immune/inflammation-related genes in the hippocampus of individuals with schizophrenia. Translational psychiatry. 2013; 3:e321. [PubMed: 24169640]

47. van Erp TG, Hibar DP, Rasmussen JM, et al. Subcortical brain volume abnormalities in 2028 individuals with schizophrenia and 2540 healthy controls via the ENIGMA consortium. Mol Psychiatry. 2015

48. Bracken BK, Rouse ED, Renshaw PF, Olson DP. T2 relaxation effects on apparent N-acetylaspartate concentration in proton magnetic resonance studies of schizophrenia. Psychiatry Res. 2013; 213:142–153. [PubMed: 23769421]

49. Sommer IE, van Westrhenen R, Begemann MJ, de Witte LD, Leucht S, Kahn RS. Efficacy of anti-inflammatory agents to improve symptoms in patients with schizophrenia: an update. Schizophr Bull. 2014; 40:181–191. [PubMed: 24106335]

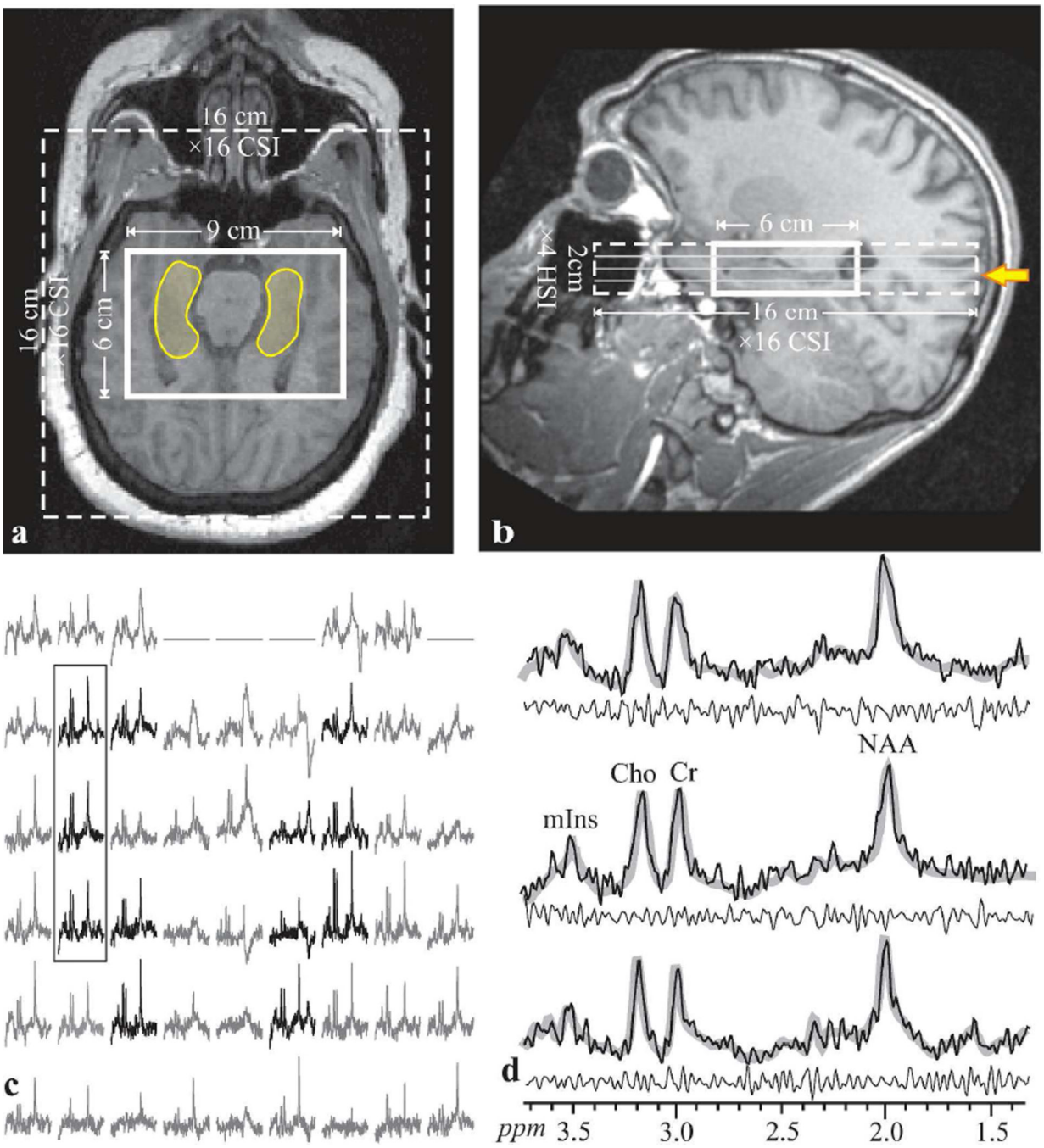

Fig. 1.

Top: Axial (**a**) and sagittal (**b**) T1-weighted MRI from a 22 year old male patient (#17 in Table 1) superimposed with the 9×6×2 cm^3 (LR×AP×IS) VOI, 16×16 cm^2 axial CSI FOV (solid and dashed lines) and the hippocampus outline (transparent yellow on **a**). The yellow arrow on **b** indicates the level of **a**, **c** and **d**.

Bottom, left, c: Real part of the 9×6 axial (LR×AP) ^1H spectra matrix from the VOI slice shown on **a** and marked with the solid yellow arrow on **b**. Spectra within the hippocampus in **a** are black, while the remaining (not included in the analyses) are gray. All are on a

common frequency (*ppm*) and intensity scale. The three spectra in the black frame over the right hippocampus are expanded on the right (**d**) for greater detail,. Note that none of the hippocampi involve voxels at the edges of the VOI (that may suffer relative VOI chemical shift displacement), the good SNR and excellent *spectral* resolution (8.1±3.0 Hz linewidth) from these high *spatial* resolution (0.5 cm^3) voxels. Right, **d**, the three spectra from the solid frame on **c** (black line) overlaid with the spectral fitt (thick gray lines) and the residual (= experimental – fit) underneath (thin black line). Note the spectral resolution and fidelity of the fit, reflected by the residual.

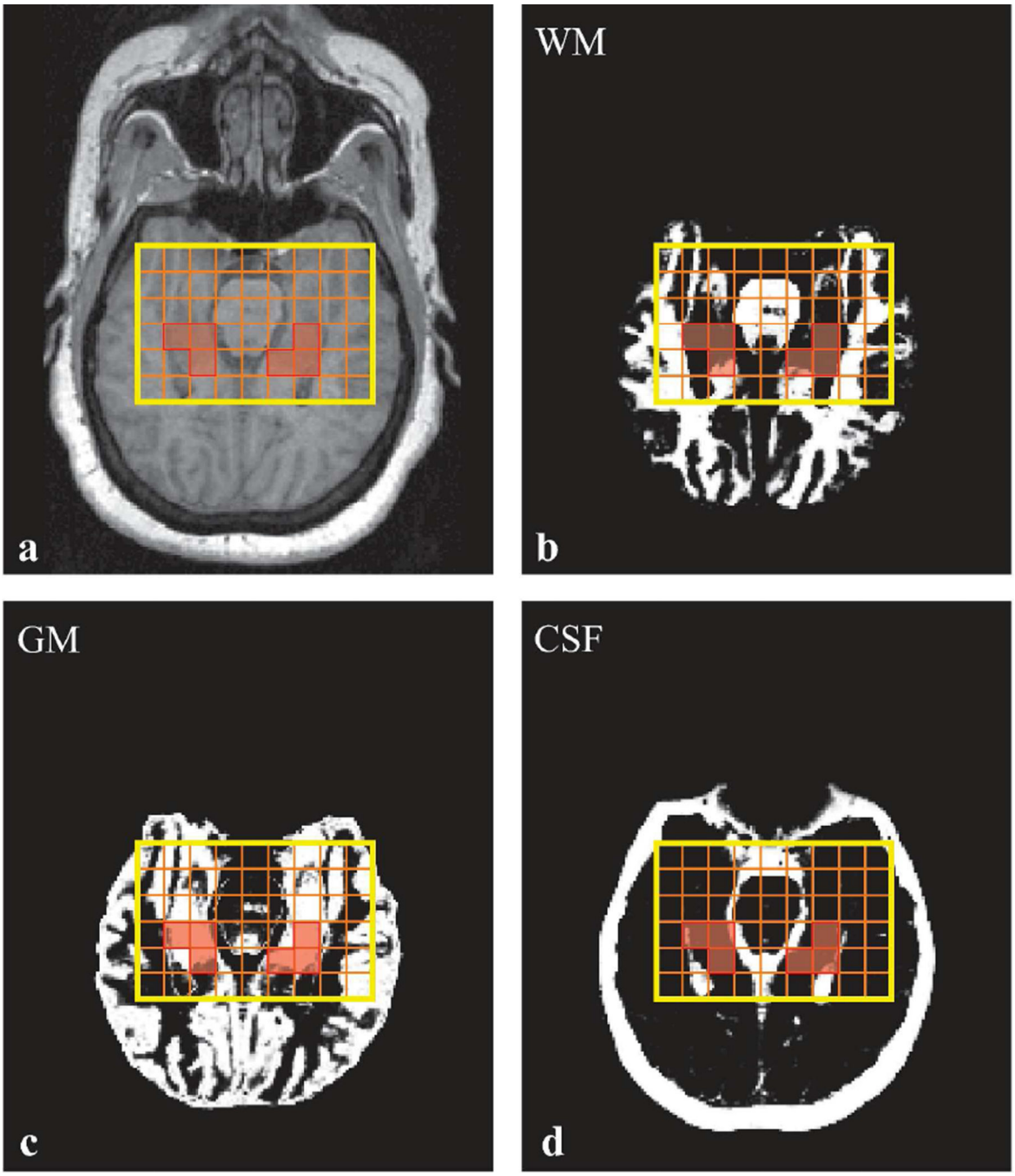

Fig. 2.

Top, **a:** Axial MP-RAGE image from a 51 year old female patient (#16 in Table 1) superimposed with the VOI (in yellow). Orange lines show the 9×6 voxels CSI grid, and voxels that passed the selection criteria to calculate the NAA concentration, highlighted in transparent red. **b, c, d:** SPM12-generated WM (**b**), GM (**c**), and CSF (**d**) masks also superimposed with the VOI CSI grid and selected voxels. Note the $n \geq 2$ voxels that "passed" the selection criteria described in the Methods.

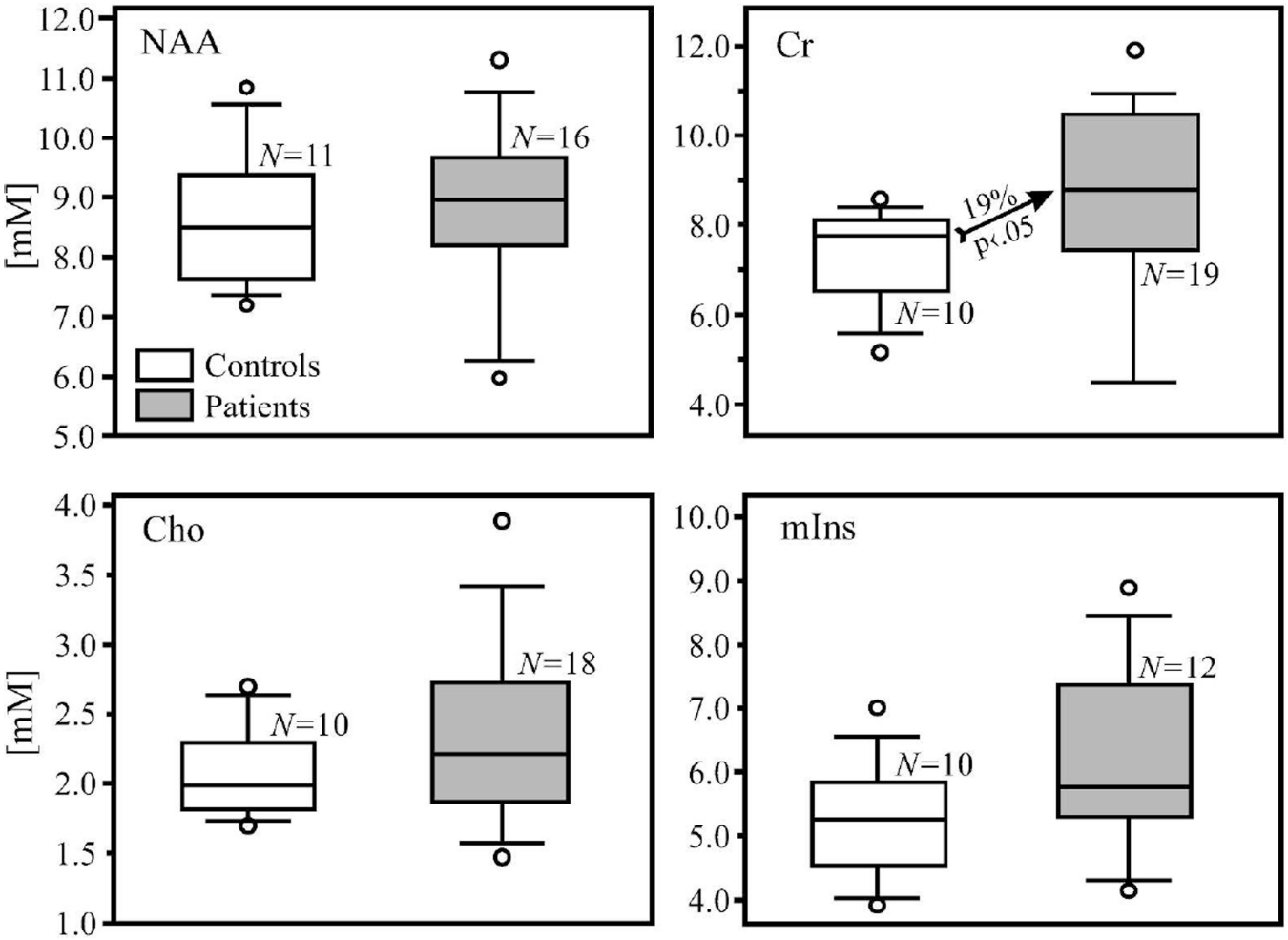

Fig. 3.

Box plots showing the first, second (median) and third quartiles, 5th and 95th percentiles (whiskers) and outliers (○) of the distribution of the bilateral hippocampal NAA, Cr, Cho, and mIns concentrations (mM) in the patients (shaded) and controls (white) boxes. Dots represent outliers. Numbers of controls and patients included in the analyses for each metabolite, *N*, are listed under boxes. Note that the NAA, Cho, and mIns concentrations do not differ significantly between patients and controls (Also see Table 2), whereas the Cr concentration is 19% higher in bilateral hippocampi of the patients than their controls (indicated by the arrow).

Table 1

Demographics for controls (C: 1 – 11) and patients (P: 12 – 30).

Subject	Status	Age[a]/Gender	Disease duration[a]	Psychotropic Medication
1	C	45/M	-	-
2	C	31/M	-	-
3	C	29/F	-	-
4	C	36/M	-	-
5	C	43/M	-	-
6	C	24/F	-	-
7	C	55/F	-	-
8	C	26/F	-	-
9	C	29/F	-	-
10	C	22/M	-	-
11	C	31/F	-	-
12	P	41/M	22	Fluphenazine
13	P	44/F	27	Quetiapine
14	P	43/M	18	Haloperidol, quetiapine
15	P	52/M	32	Citalopram
16	P	51/F	15	Gabapentin, lithium, ziprasidone
17	P	23/M	3	Risperidone
18	P	47/M	31	Fluoxetine, risperidone, valproic acid, trazodone
19	P	44/M	26	Clozapine, valproic acid
20	P	26/M	8	Ziprasidone
21	P	29/F	8	Buproprion, aripiprazole, fluphenazine
22	P	42/F	23	Ziprasidone, buproprion, eszopiclone
23	P	22/M	4	Clozapine
24	P	48/M	23	Quetiapine
25	P	34/M	5	Risperidone
26	P	30/F	10	Risperidone
27	P	49/F	31	Aripiprazole
28	P	51/F	35	NA
29	P	43/F	20	Aripiprazole, escitalopram, fluphenazine
30	P	52/M	30	Aripiprazole, valproic acid, hydroxyzine, paroxetine, trazodone

[a]Years, "-"=not applicable.

Table 2

Metabolite	Controls	Patients	*p*-value
NAA	[a]8.7±1.2 (n=11)	[a]8.8±1.6 (n=16)	0.876
Cr	**[a]7.4±1.2 (n=10)**	**[a]8.7±2.2 (n=19)**	**0.035**
Cho	[a]2.1±0.3 (n=10)	[a]2.3±0.7 (n=18)	0.189
mIns	[a]5.2±0.9 (n=10)	[a]6.1±1.5 (n=12)	0.161
Volume (cm^3)	**8.4±0.5 (n=11)**	**7.5±0.9 (n=19)**	**0.003**

Means ± Standard deviation, number of subjects from whom the data was derived *n* (in parentheses), and *p*-values (from unequal variance T tests) of the absolute NAA, Cr, Cho and mIns hippocampal GM concentrations [a](millimolar), as well as the volumes of the bilateral hippocampi in controls and patients (in cm^3). Significant differences are in boldface; note elevation of Cr and reduction in volume in patients compared to controls.